Image Cover Sheet

CLASSIFICATION	SYSTEM NUMBER
UNCLASSIFIED	508290

TITLE

NON-DESTRUCTIVE MAPS OF STRESS CONCENTRATION EFFECTS NEAR NOTCHES

System Number:

Patron Number:

Requester:

Notes:

DSIS Use only:

Deliver to:

Non-destructive Maps of Stress Concentration Effects near Notches

J. Root and J. Katsaras
National Research Council, Canada
Chalk River Laboratories
Chalk River, Ontario, Canada K0J 1J0

J. Porter
Defence Research Establishment Atlantic
P.O. Box 1012
Dartmouth, Nova Scotia, Canada B2Y 3Y8

Email: John.Root@nrc.ca
http://neutron.nrc.ca/

Abstract

Recent advances in neutron detector technology and the ability of neutrons to penetrate through many millimetres of most engineering materials have made it feasible to investigate the effects of stress-concentration near notches. To demonstrate this capability, the development of the strain field near a sharp notch in an HY-100 steel bar is scanned as a three-point bending load is increased to the point of metal-tearing. On unloading, residual stresses are scanned. As a second demonstration, the stress-concentration effects of a blunt notch in a tensile test specimen are presented. These measurements are performed at a temperature of 250 °C, which is maintained by a heater that surrounds the specimen. In both examples, the gradients of the strain distribution are substantial, but neutron diffraction has a sufficient spatial resolution to characterize the effects of stress concentration quantitatively.

1 Nomenclature

2θ	scattering angle, in diffraction, at a particular location in a specimen	[degrees]
$2\theta_o$	scattering angle in stress-free material	[degrees]
ε	crystal lattice strain	[m/m]
r	distance from the root of a notch or the tip of a crack	[m]

2 Introduction

Non-destructive strain measurements are made by neutron diffraction to scan the internal distribution of stresses in intact engineering components, such as bent tubes [1], weldments [2] and shrink-fit cylinders [3]. Because it is non-destructive, the neutron-diffraction strain-scanning technique can track the development of the elastic strain field in a single specimen as applied load is increased. Neutron beams can also penetrate through heating elements to scan the strain distribution in specimens that are held at the temperatures of an operating plant.

By characterizing the effects of load and temperature on internal stress distributions, one may begin to address fundamental issues of the fitness-for-service of critical engineering components. For this paper, a notched bar of HY-100 steel was subjected to three-point bending to the point of metal tearing and neutron diffraction traced the evolution of the strain distribution near the notch. The HY-100 material is found in marine structures, where a robust response to plastic deformation and crack formation is needed. Also for this paper, neutron diffraction scans were made of the strain distribution below a semi-circular groove in a tensile specimen of Zr-2.5Nb, held at a temperature of 250 °C. This experiment begins to investigate the stress-concentration effects of fretting flaws or corrosion pits that might appear in pressurized piping systems.

Incident and diffracted neutron beams intersect to form a small "sampling volume" that is scanned through a raster of locations inside a component. At each location, a diffraction peak is acquired, the mean scattering angle (2θ) is determined, and the crystal-lattice strain, ε, is determined by comparison with the scattering angle for stress-free material ($2\theta_o$), through the relation:

$$\varepsilon = \frac{\sin\theta_o}{\sin\theta} - 1. \qquad (1)$$

Unlike a mechanical strain gauge, this crystal lattice strain is related only to the stresses in crystallites and is not directly sensitive to plastic strain. Typical incident neutron beam fluxes lie in the range of (0.5 - 5) x 10^4 neutrons/mm^2/s and the fraction of this weak neutron beam that is diffracted towards a detector is typically less than 1 part in 1000 in polycrystalline materials. A challenge in neutron strain-scanning is to optimize the rate at which data can be collected while retaining a sufficient spatial resolution to characterize stress-gradients adequately. These stress gradients are particularly steep when approaching stress-concentrators. For example a thin plate, deformed elastically, has an intensified stress that increases by a factor of $1/r^{1/2}$ as the distance to a notch tip, r, is reduced. [4].

3 Neutron Diffractometer

The L3 neutron diffractometer is situated at the NRU reactor, a medium-flux source of thermal neutrons, located at Chalk River Laboratories in Canada. The diffractometer is equipped with a 32-element multiwire ^{3}He detector that spans 2.7° in 2θ, and can acquire a complete diffraction peak in one setting. The specimen table is equipped with computer-controlled XYZ translators that can handle large loads. To apply three-point bending loads to the notched HY-100 bar, a screw-driven clamp, which weighed more than 100 kg, was attached to the translator so the specimen-plus-clamp could be positioned during strain scanning. Tensile loads were applied to the Zr-2.5Nb specimen by a universal testing machine with a capacity of 50 kN. [5] The testing machine was also mounted on the translator system for scanning of strain within the loaded specimen. The incident and diffracted neutron beams were defined by slits in neutron-absorbing

cadmium masks. Slit dimensions were chosen to optimize the trade-off between spatial resolution and signal intensity for each experiment.

4 HY-100 Notched Bar in Three-Point Bending

4.1 Experimental Details

A sketch of the three-point bending specimen is shown in Fig. 1. The bar was about 16 mm thick, 38 mm in the vertical direction and 220 mm in the longitudinal direction. The bar was oriented such that the longitudinal component of strain was measured. The bending loads were applied in the vertical direction through large-diameter pins. An overall measure of distortion was monitored by a strain gauge attached to the bottom surface of the bar. Strains were determined from shifts in 2θ of the (110) diffraction peak from the body-centered cubic crystal structure of the HY-100 steel. The stress-free value, $2\theta_o$, was determined from measurements in the bar prior to the application of load. The sampling volume had dimensions 1.5 mm x 1.5 mm x 2 mm, with the long dimension parallel to the vertical direction. The raster of measurement locations extended upwards from the root of a sharp notch and to one side. All measurements were made at mid-thickness of the bar. Strain scans were made with strain-gauge readings that included 10.0×10^{-4} (mainly elastic deformation), 16.2×10^{-4} (plastic zone developing), 16.7×10^{-4} (internal crack develops), and finally 0.0 (residual stresses).

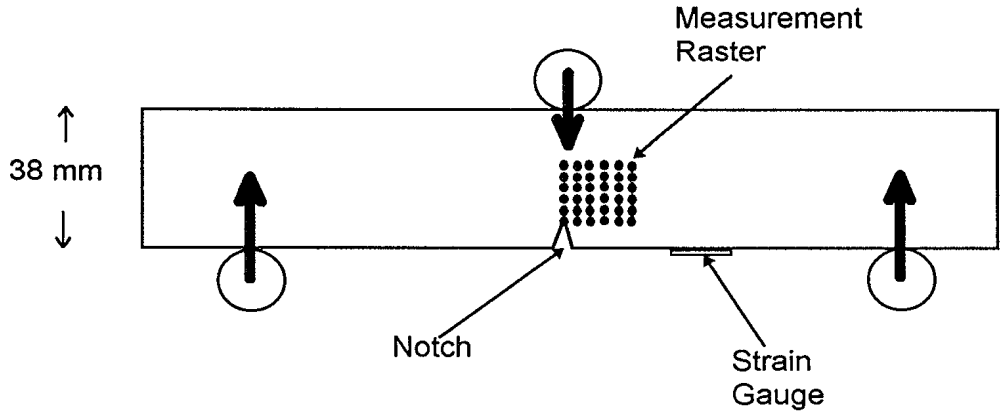

Figure 1. **Sketch of notched HY-100 bar in three-point bending configuration.**

4.2 Results for Various Bending Loads

Maps of the longitudinal component of strain versus distance from the original notch tip are presented in Fig. 2. Note in these plots that the maximum vertical distance from the notch tip corresponds approximately to the neutral axis of the bent bar, not to the top surface of the bar. A characteristic "butterfly" pattern of elastic strain is well-developed with low deformation of the bar (Fig. 2a). A maximum strain value, 25×10^{-4}, occurs about 3 mm above the notch, but values close to this maximum extend towards the tip of the notch. On increasing the bend to a point that significant plasticity occurs (Fig. 2b), the maximum strain increases to about 40×10^{-4} and remains at the same distance from the original notch tip. This strain maximum is more localized than was observed at the lower load. On approach to the original notch tip there is a factor-of-two reduction of lattice strain, which is a consequence of plasticity near the notch.

Increasing the bend still further (Fig. 2c), there is a dramatic shift of the strain maximum away from the original notch tip. This shifted pattern of strain, measured at mid-thickness of the bar, suggests the presence of an internal crack. The crack could not be seen at the surface of the bar, but the near-zero longitudinal strain, which appears at the location of the original notch tip, supports the idea that an internal crack was formed. (The stress normal to a crack surface is zero, and the crystal lattice strains measured in the same direction would be close to zero, as observed.) When a similar bar was bent slightly beyond the deformation indicated as 16.7×10^{-4} on the strain gauge, a metal tear appeared clearly on the surface. Unloading the bar from the condition in (Fig. 2c), a residual strain pattern was obtained (Fig. 2d). Along the line directly above the notch, one observes the classic residual-strain pattern of a bent plate. This bent-plate pattern is confined to the region below the notch. As little as 15 mm away in the longitudinal direction, it appears as if no plastic deformation has occurred at all.

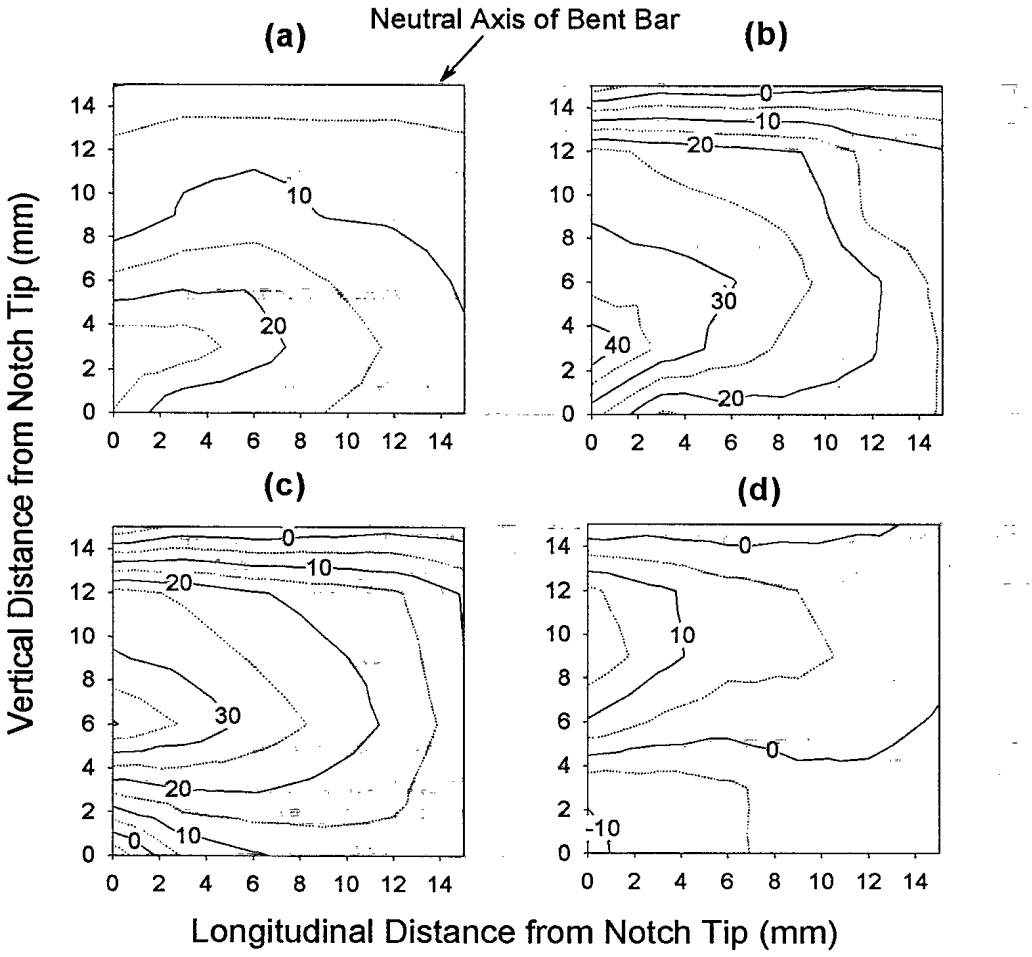

Figure 2. **Maps of longitudinal strain (10^{-4}), at various loading conditions: a) 10×10^{-4}, b) 16.2×10^{-4}, c) 16.7×10^{-4} and d) unloaded after 16.7×10^{-4}.**

5 Zr-2.5Nb Tensile Specimen with a Blunt Notch

5.1 Experimental Details

A sketch of the tensile specimen is shown in Fig. 3. The specimen was 4 mm thick, 6.5 mm wide, and had a gauge length of 50 mm. A semi-circular groove of radius 1 mm extended across the width of the specimen. The testing rig and specimen were oriented such that the component of strain parallel to the tensile axis was measured. The applied stress was monitored by a load cell. The temperature was held at 250 °C, and monitored by a type-K thermocouple in good thermal contact with the specimen. Strains were determined from shifts in 2θ of the $(20\bar{2}0)$ diffraction peak from the hexagonal close-packed crystal structure of the zirconium alloy. The stress-free value, $2\theta_o$, was determined from measurements in the specimen at 250 °C, prior to the application of load. The sampling volume had dimensions 0.5 mm x 0.5 mm x 5 mm, with the long dimension parallel to the groove. This configuration ensured high spatial resolution of strain gradients as measurements were made along a line below the root of the groove. Strain scans were made with two settings of the nominal stress (ie the applied load divided by the cross sectional area below the groove): 300 MPa and 450 MPa.

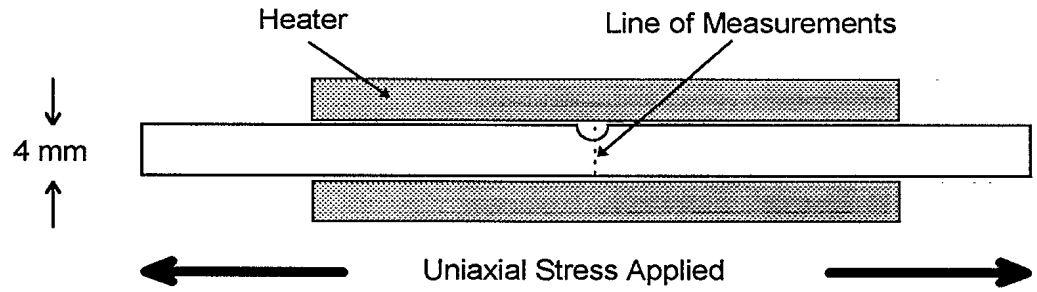

Figure 3. **Sketch of Zr-2.5Nb tensile specimen with semi-circular groove.**

5.2 Results of Tensile Loading

The variation of longitudinal strain with depth below the root of the groove is presented in Fig. 4. Results for two values of nominal stress are compared, both obtained at a constant temperature of 250 °C. At this temperautre, the elastic limit of the stress-strain curve is about 330 MPa. A nominal stress of 300 MPa would place the material in the region of elastic response, but the blunt notch generates a stress concentration that is evident in the increased strain on approach to the root of the groove. The linear form of the strain distribution is similar to the stress-concentration curve expected in plane-strain geometry. [4] The stress-concentration factor for this specimen geometry is about 1.7. [6] The material closest to the blunt notch is therefore affected by plasticity, which explains the saturation of the strain value at depths less than 1 mm from the root of the groove. At a nominal stress of 450 MPa, there is some degree of plasticity at all depths below the groove.

6 Conclusions

Neutron diffraction provides opportunities to investigate the interior response of engineering materials to conditions of load and temperature, even in the presence of stress-concentrators, such as notches, cracks and blunt indentations. With a medium-flux research reactor and a multi-wire

detector, there is enough signal intensity to achieve the spatial resolution needed to characterize stress-concentration effects.

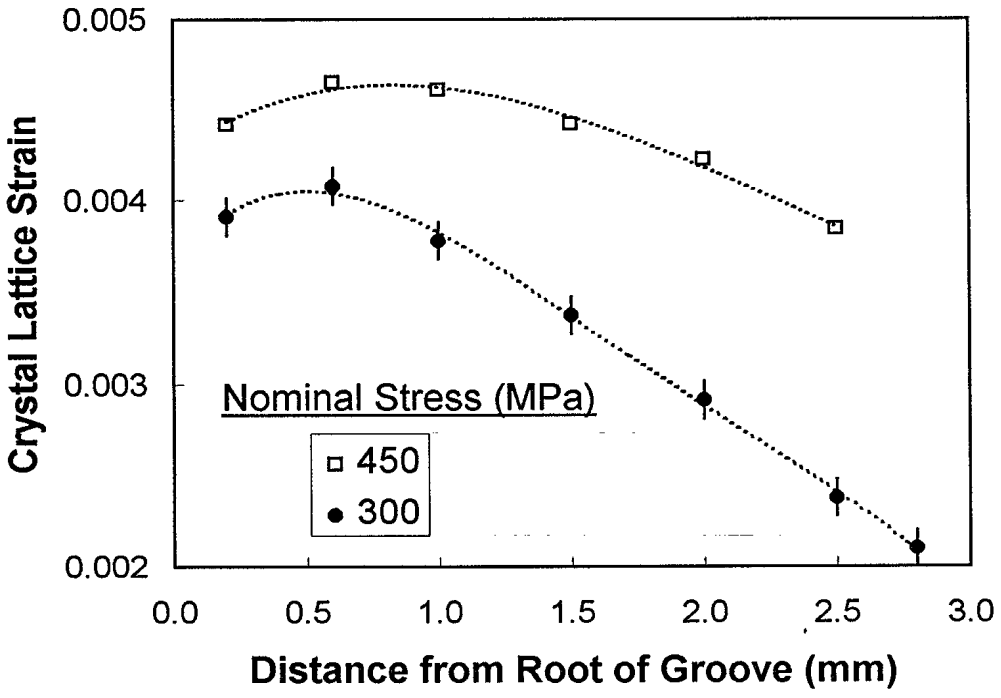

Figure 4. **Variation of longitudinal strain with depth below the root of a groove in a Zr-2.5Nb tensile specimen. Typical uncertainties shown as vertical bars, ±σ.**

7 Acknowledgements

These challenging neutron strain-scanning projects were made possible with the skillful technical assistance of J. Fox, D. Tennant, M. Montaigne, L. McEwan, M. Potter, J. Bolduc.

8 References

1. T.M. Holden, R.A. Holt, G. Dolling, B.M. Powell, J.E. Winegar, *Met. Trans.* **19A** (1988), 2207-2214.
2. J.H. Root, T.M. Holden, J. Schröder, C.R. Hubbard, S. Spooner, T.A. Dodson and S.A. David, *Mat. Sci. and Tech.* (1993), 754-759.
3. T. Lorentzen and E.B. Nielsen, "Neutron Diffraction Strain Measurements on Shrink-fit Ring Assembly", in *Proc. Fourth Int. Conf. On Residual Stresses,* June 8-10, 1994, Society for Experimental Mechanics, Inc., Bethel, CT, 06801, USA.
4. G.E. Dieter, *Mechanical Metallurgy*, McGraw-Hill, Inc., New York, 1986.
5. Applied Test Systems, Inc., 348 New Castle Rd., Box 1529, Butler, PA. 16003
6. R.E. Peterson, *Stress Concentration Factors*, John Wiley and Sons, New York (1974).

#508290